International Journal of Scientific Engineering and Science
Volume 10, Issue 1, pp. 40-47, 2026. ISSN (Online): 2456-7361

Robust Background Suppression of Weld Bead Images Under Nonuniform Illumination and Metallic Reflections

Linda Marlinda[1*], Marysca Shintya Dewi[2]
[1]Informatika, Universitas Nusa Mandiri, Jakarta, Indonesia-13620
[2]Teknik Mesin, Universitas Dian Nusantara, Jakarta, Indonesia-17433

Abstract**—***Analysis of weld bead images in industrial environments often encounters challenges such as uneven illumination, strong metallic reflections, shadows, and background textures that closely resemble the weld bead. This study proposes a classical image processing workflow for background suppression in weld bead images by integrating flat field correction, contrast enhancement, adaptive morphological operations, region of interest ROI band selection, and marker controlle watershed segmentation based on distance transforms. The proposed approach is evaluated using entropy, Structural Similarity Index Measure SSIM, and Gray Level Co occurrence Matrix GLCM contrast. Experimental results show that the global image entropy decreases from 6.88 to 3.75, indicating a reduction in background complexity. At the same time, the SSIM value within the ROI remains at 1.00, and the GLCM contrast remains stable at 7.09, confirming that the structural integrity and textural characteristics of the weld bead are preserved. The results also indicate that complete background removal using low level classical techniques remains challenging when background intensity and texture closely mimic the weld bead. Therefore, the proposed method is best characterized as a robust background suppression framework rather than a full background removal solution.*

Keywords**—** *Weld bead imaging, Background suppression, Morphological image processing, Watershed segmentation, Quantitative image evaluation.*

I. Introduction

Manufacturing industries prioritize weld quality assessment to guarantee structural integrity and operational safety. However, current practices largely rely on manual visual inspection to detect defects. This method inherently produces inconsistent results due to operator subjectivity and fatigue [1][2]. Therefore, researchers actively investigate automated image base systems to enhance inspection reliability and efficiency.

Despite technological advances, industrial environments frequently present adverse imaging conditions. Visible light cameras often capture non uniform illumination, strong metallic reflections, and complex background textures[3], [4]. These factors degrade the performance of classical image processing techniques. Specifically, such conditions hinder background removal and negatively impact critical downstream tasks like feature extraction.

Previous studies explored preprocessing strategies, including grayscale normalization and morphological filtering, to improve visibility[4][5]. These methods demonstrate limited effectiveness under severe lighting variations. Background regions often mimic the intensity and texture characteristics of the weld bead itself [6]. Consequently, basic low-level techniques struggle to achieve complete background removal in real world scenarios.

To address these challenges, this study prioritizes a robust classical image processing framework due to its inherent simplicity and transparency. The proposed approach targets background suppression rather than complete semantic removal [7]. This strategy reduces noise while preserving the weld bead structural integrity. Thus, it provides a stable foundation for inspection without relying on complex computational frameworks.

The proposed workflow integrates flat field correction, gradient based ROI selection, and marker driven watershed segmentation. Subsequently, the analysis evaluates the pipeline effectiveness using entropy, Structural Similarity Index (SSIM), and Gray Level Co Occurrence Matrix (GLCM) contrast [8], [9].

II. Literature Review

A. Structural Background Interference in Weld Bead Images

Structural background interference is a persistent challenge in two-dimensional (2D) image analysis, especially in weld bead imaging under real-world industrial conditions[10]. It occurs when background regions share geometric, textural, or intensity characteristics with the weld bead, complicating reliable foreground isolation. Typical sources include surface texture, nonuniform illumination, cast shadows, and metallic reflections during image acquisition[11]. When not properly suppressed, these structures overlap with object boundaries and undermine the reliability of subsequent stages such as segmentation and quantitative feature extraction.

Previous studies indicate that background interference is not merely visual noise but a structural disturbance that disrupts object continuity and representation. Residual patterns may introduce false edges, distort shapes, and bias texture measurements, thereby reducing the reliability of image analysis.

B. Intensity-Based and Conventional Background Removal Techniques

Early background removal approaches primarily relied on pixel-level intensity discrimination. Global and adaptive thresholding techniques separate foreground and background based on fixed or locally adaptive intensity values, offering

simplicity and low computational cost. The methods are highly sensitive to illumination variations and fail when foreground and background intensity distributions overlap[11]. Linear filtering techniques, such as Gaussian and median filtering, have also been employed to smooth background noise, but they often blur object boundaries and are ineffective against structured background patterns[12].

Although adaptive thresholding and region-based techniques improve local robustness under varying illumination, they remain fundamentally limited when background structures share similar intensity and texture characteristics with the weld bead. As a result, conventional intensity-driven approaches are insufficient for handling complex structural background interference in weld bead images.

C. *Learning Based Segmentation and Practical Constraints*

Recent studies highlight learning based methods, including machine learning and deep learning models, for background removal and semantic segmentation. Convolutional neural networks can effectively segment weld regions and detect defects when trained on large annotated datasets, often producing clean results comparable to commercial applications. Despite these advantages, such approaches demand extensive labeled data, high computational resources, and careful optimization, while their opaque decision processes reduce interpretability and controllability critical requirements in industrial inspection[13].

D. *Morphological Image Processing for Structural Feature Preservation*

Morphological image processing provides a classical and interpretable framework for analyzing image structures based on shape and spatial relationships. Rooted in mathematical morphology, this approach employs fundamental operators such as erosion and dilation, as well as compound operations including opening and closing, to manipulate image regions according to their geometric properties[14].

Unlike intensity driven or data driven approaches, morphological processing explicitly targets structural characteristics rather than pixel values alone. By designing appropriate structuring elements, morphological operators can selectively suppress background patterns while preserving the continuity and shape of the foreground object. This structural focus makes morphological processing particularly suitable for weld bead images, where foreground and background often differ more in geometry than in intensity[13], [14].

E. *Morphological-Based Background Suppression Strategies*

Morphological techniques have been widely employed as supporting components in segmentation pipelines, often combined with thresholding or region-based methods[15]. The role is frequently limited to post processing rather than being treated as a central strategy for background suppression. In recent studies, marker-controlled watershed segmentation has been introduced to improve region separation by guiding segmentation using predefined foreground and background markers[16].

The effectiveness of watershed-based segmentation is highly dependent on the quality of marker generation. Distance transform based interior markers have been shown to provide robust representations of object cores, reducing over-segmentation and sensitivity to noise. When integrated with morphological preprocessing, such strategies can enhance the stability of segmentation results under complex background conditions.

III. METHODOLOGY

This section presents the proposed classical image processing pipeline for background suppression in weld bead images under nonuniform illumination and metallic reflections. Figure 1 summarizes the workflow, which integrates illumination normalization, contrast enhancement, morphological processing, distance transform based marker extraction, and marker controlled watershed segmentation. The following subsections describe each stage sequentially to explain how the final results are obtained and how the method can be applied in practice [6], [17], [18], [19], [20], [20], [21], [21] .

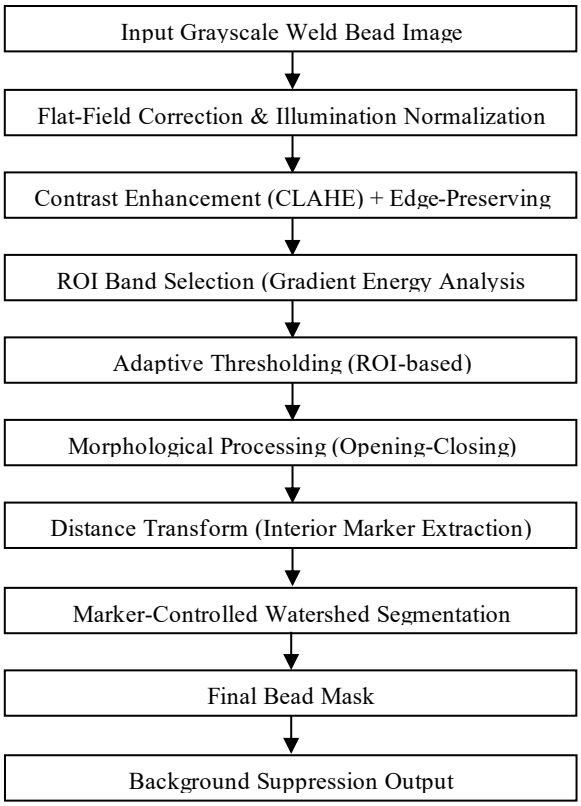

Fig. 1. Morphological-Based Background Suppression Workflow

A. *Image Acquisition and Problem Setting*

This study utilizes a dataset of grayscale weld bead images sourced from Pinterest.com to represent real industrial environments. These images exhibit non-uniform illumination, strong metallic reflections, and background textures similar to the weld bead. Consequently, these conditions necessitate a robust background suppression strategy to overcome the limitations of classical removal techniques.

Let $I(x,y)$denote the original grayscale weld bead image acquired under non-uniform illumination, metallic reflections, shadows, and textured background. The objective of this study is to suppress background interference while preserving the structural and textural integrity of the weld bead.

B. Preprocessing and Illumination Normalization

The preprocessing stage applies flat-field correction to mitigate global illumination inconsistencies. Subsequently, the algorithm employs Contrast-Limited Adaptive Histogram Equalization (CLAHE) to enhance local contrast while preventing noise amplification. Finally, edge-preserving filtering reduces noise without degrading the essential bead boundaries.

To compensate for non-uniform illumination, flat-field correction is applied by estimating the background illumination $B(x,y)$ using large-kernel Gaussian smoothing:

$$B(x,y) = G_\sigma * I(x,y)$$

where G_σ denotes a Gaussian kernel with a large standard deviation σ.

The normalized image $I_n(x,y)$ is then obtained as:

$$I_n(x,y) = \frac{I(x,y)}{B(x,y)+\epsilon}$$

where $\epsilon$is a small constant to avoid division by zero.

C. Contrast Enhancement and Noise Reduction

Local contrast enhancement is performed using Contrast Limited Adaptive Histogram Equalization (CLAHE), which redistributes pixel intensities within local tiles while limiting contrast amplification to suppress noise. An edge-preserving filter is subsequently applied to reduce noise while preserving bead boundaries, ensuring stability for downstream morphological operations.

D. ROI Band Selection Based on Gradient Energy

The system automatically determines a Region-of-Interest (ROI) band to localize the weld bead. Specifically, the algorithm analyzes column-wise gradient energy to identify the dominant vertical structure. This process selects a vertical band to restrict subsequent processing to the relevant region and suppress irrelevant background areas.

Local contrast enhancement is performed using Contrast Limited Adaptive Histogram Equalization (CLAHE), which redistributes pixel intensities within local tiles while limiting contrast amplification to suppress noise. An edge-preserving filter is subsequently applied to reduce noise while preserving bead boundaries, ensuring stability for downstream morphological operations.

The column-wise gradient energy $E(x)$is calculated as:

$$E(x) = \frac{1}{H}\sum_{y=1}^{H} |G_x(x,y)|$$

where H is the image height.

The column corresponding to the maximum gradient energy defines the center of the vertical Region-of-Interest (ROI) band, which constrains further processing to the most relevant region.

E. Morphological Processing and Coarse Mask Generation

Within the ROI band, adaptive thresholding is applied to generate an initial coarse mask. Morphological closing and opening operations are then performed to reduce noise, fill small gaps, and stabilize the bead region. Connected component analysis with geometric constraints is used to retain the dominant bead-like structure.

Within the ROI band, adaptive thresholding is applied to generate a coarse binary mask $M(x,y)$. Morphological closing and opening are then used to stabilize the bead region:

$$M_{close} = (M \oplus S) \ominus S$$
$$M_{open} = (M_{close} \ominus S) \oplus S$$

where $\oplus$and $\ominus$denote dilation and erosion, respectively, and $S$is a structuring element.

Connected component analysis is employed to retain the dominant bead-like region based on area and aspect ratio constraints.

F. Distance-Transform–Guided Marker Generation

To obtain reliable interior markers, a distance transform is computed on the coarse bead mask. Local maxima of the distance map are selected as sure foreground markers representing the interior of the weld bead, while dilated inverse regions are used to define sure background markers. This marker configuration reduces sensitivity to reflections and shadows.

To generate reliable interior markers, the Euclidean distance transform $D(x,y)$is computed on the refined binary mask:

$$D(x,y) = \min_{(x',y')\in\partial M} \sqrt{(x-x')^2 + (y-y')^2}$$

Local maxima of $D(x,y)$are selected as sure foreground markers M_f, representing the interior of the weld bead. Sure background markers M_b are obtained from dilated inverse regions.

G. Marker-Controlled Watershed Segmentation

Marker-controlled watershed segmentation is performed on the gradient magnitude image within the ROI band. The distance transform based foreground markers guide region growth toward the bead interior, while background markers prevent over-segmentation into surrounding regions. The resulting segmentation yields a refined bead mask used for background suppression.

Watershed segmentation is performed on the gradient magnitude image $G(x,y)$, defined as:

$$G(x,y) = \sqrt{G_x(x,y)^2 + G_y(x,y)^2}$$

Using markers $M_f$and M_b, marker-controlled watershed segmentation partitions the ROI into foreground and background regions. The resulting segmentation produces a refined weld bead mask $M_w(x,y)$, which is used for background suppression.

H. Quantitative Evaluation

The effectiveness of the proposed pipeline is evaluated using entropy, Structural Similarity Index Measure (SSIM), and Gray Level Co-occurrence Matrix (GLCM) contrast. Entropy assesses global background complexity, SSIM evaluates

International Journal of Scientific Engineering and Science
Volume 10, Issue 1, pp. 40-47, 2026. ISSN (Online): 2456-7361

structural preservation relative to the original image, and GLCM contrast measures texture separability. Metrics are computed at both full-image and ROI-band levels to distinguish global background suppression from local structural preservation.

1) Entropy

Global image complexity is measured using Shannon entropy:

$$H = -\sum_{i=0}^{L-1} p(i) \log_2 p(i)$$

where $p(i)$is the probability of gray level $i$and $L$is the number of intensity levels.

2) Structural Similarity Index Measure (SSIM)

Structural preservation is evaluated using SSIM:

$$\text{SSIM}(I, I') = \frac{(2\mu_I\mu_{I'} + C_1)(2\sigma_{II'} + C_2)}{(\mu_I^2 + \mu_{I'}^2 + C_1)(\sigma_I^2 + \sigma_{I'}^2 + C_2)}$$

where μ, σ, and $\sigma_{II'}$ denote mean, variance, and covariance terms, respectively.

3) GLCM Contrast

Texture separability is quantified using GLCM contrast:

$$\text{Contrast} = \sum_{i,j} (i-j)^2 P(i,j)$$

where $P(i,j)$represents the normalized gray-level co-occurrence probability.

IV. Results and Discussion

A. Image Preprocessing

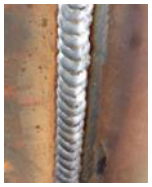

Fig. 1. Original Image

The original image presents a weld bead on a metal plate with a visually complex background. The background contains color variations, oxidation marks, grinding traces, and uneven illumination. The weld bead appears as a bright gray structure with a consistent overlapping pattern, yet its visual separation from the background remains limited. The RGB image is converted into grayscale by projecting color information into a single intensity channel. Each pixel is represented by its luminance value, which reflects light energy rather than color. This conversion removes background color variations, preserves intensity contrast between the weld bead and the base plate, and simplifies the image from three channels to one. The resulting grayscale image maintains the structural integrity of the weld bead, reduces background complexity, and prepares the data for subsequent processing stages such as intensity normalization, initial masking, and morphological operations.

1. The intensity normalization process (before–after)

The intensity normalization process was applied directly to the grayscale image to improve contrast uniformity and visual clarity. Prior to normalization, the intensity distribution remained uneven, with certain background regions appearing excessively dark while the weld bead exhibited overly bright saturation. Local contrast between the weld bead and the background was inconsistent, particularly around grinding marks and oxidation stains. After normalization, the intensity became more evenly distributed across the image. The weld bead retained its dominance as a high-intensity region without excessive saturation, and the background appeared more homogeneous, reducing visual interference. Edge transitions between the weld bead and the base plate became clearer and more stable, facilitating subsequent segmentation and feature extraction.

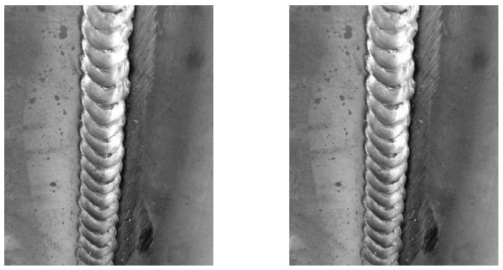

Fig. 2. (a) before normalization Grayscale (b) After Intensity Normalization

2. Initial masking based on grayscale normalization results

Fig. 3. (a) Normalized Grayscale, (b) Initial Mask (Adaptive Theshold) , (c) Masked Image

The initial masking stage was performed on the intensity-normalized grayscale image to isolate the weld bead from the background. The input image exhibited improved contrast stability compared to the original grayscale, allowing clearer differentiation between object and background. Adaptive thresholding was applied to emphasize high-intensity regions associated with the weld bead and suppress inconsistent low-intensity areas in the background. This method was selected due to the non-uniform illumination, which renders global thresholding ineffective. The resulting binary mask roughly segmented the weld bead while retaining background noise in the form of speckles and coarse textures. When applied to the grayscale image, the mask preserved the weld bead structure and reduced background interference. Although non-relevant areas remain, the image is now suitable for further refinement through morphological operations.

B. Morphological-Based Processing

Fig. 4. (a) Initial Mask (before erosion), (b) After Erosion), (c) Masked image after erosion

International Journal of Scientific Engineering and Science
Volume 10, Issue 1, pp. 40-47, 2026. ISSN (Online): 2456-7361

The erosion stage was applied to the binary mask generated from the intensity-normalized grayscale image. The initial mask still contained small white speckles, fine background textures, and non-relevant fragments surrounding the weld bead. Erosion was performed using a small elliptical structuring element (3×3) with a single iteration to remove spatially weak noise, thin out non-representative white regions, and suppress residual background textures. This operation selectively eroded foreground pixels at edges and small areas, preserving only spatially continuous structures. As a result, most background noise was eliminated, and the weld bead remained intact due to its spatial coherence. The refined mask became more focused on the main object, and when reapplied to the grayscale image, it produced a cleaner and more isolated weld bead. Although some edge thinning occurred, the structural details were preserved, making the output suitable for subsequent dilation or opening to restore weld bead thickness.

1. Results of the dilation stage to restore the thickness of the weld bead structure after erosion

Fig. 5. (a) After erosion (input to dilation), (b) After Dilation, (c) Masked Image after dilation

The dilation stage was applied to the binary mask resulting from the erosion process, where the weld bead structure had been partially thinned but was already free from most background noise. Using a small elliptical structuring element (3×3) with one iteration, dilation aimed to restore the thickness of the weld bead, reconnect minor gaps, and reinforce the continuity of its shape. This morphological operation adds pixels to the foreground, allowing previously eroded regions to be reconstructed. As a result, the weld bead appeared thicker and more stable, with clearer contours and reduced fragmentation. Although minor noise may re-emerge, its intensity remains lower than in the initial mask. The final masked image shows a well-defined weld bead with suppressed background interference, providing a robust foundation for subsequent operations such as opening or closing.

2. Opening (Erosion + Dilation as one package for more stable noise cleaning)

Fig. 6. Initial Mask (Before Opening), (B) After Opening (Erode+Dilater), (C) Masked Image After Opening

The opening operation was applied to the binary mask obtained from the normalized grayscale image to improve segmentation quality. This process combined erosion and dilation sequentially to remove small noise, suppress background fragments, and preserve the continuity of the weld bead structure.

The results show that unstable noise was effectively reduced while the weld bead remained intact and more focused. The refined mask highlights the weld bead as the dominant object, with background interference significantly diminished. The masked image appears cleaner and clearer, providing a stable foundation for the next stage, namely closing, which will further refine the weld contour and seal minor gaps.

3. Closing (closing small gaps in the weld bead + improving object continuity)

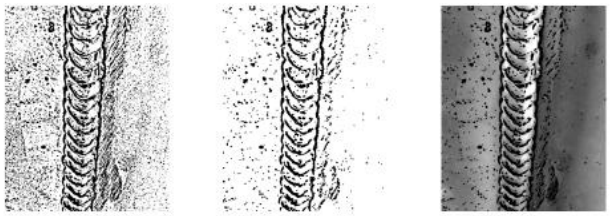

Fig. 7. (a) After opening (Input to Closing), (b) After Closing (Dilate + Erode), (c) Masked Image After Closing

The closing operation was applied to the binary mask resulting from the opening stage to enhance structural continuity and eliminate small gaps within the weld bead. This process involved dilation followed by erosion to reconnect thin, fragmented regions and smooth the foreground boundaries.

The input mask already exhibited reduced noise and improved stability, yet small discontinuities and residual artifacts remained. After closing, the weld bead structure became more cohesive, with minor gaps effectively sealed and contours appearing more solid. The refined mask showed improved clarity and readiness for feature extraction.

In the final masked image, the weld bead appeared more dominant with sharper boundaries, while the background was further suppressed. The overlapping pattern of the bead remained visible, now with enhanced continuity. This output provides a robust foundation for the final stages, including background removal and quantitative evaluation using metrics such as Entropy, SSIM, and GLCM Contrast.

4. Final Background Suppression Result

Fig. 8. (a) Original Grayscale, (b) Final Mask, (c) Final Background Removal Result

The final background removal was performed by applying the closing-stage mask to the intensity-normalized grayscale image. This mask was already stable, continuous, and focused on the weld bead structure with minimal noise. Bitwise masking was used to retain only the pixels within the weld bead region while suppressing all background pixels outside the mask.

The original grayscale image contained complex background textures, including plate marks, stains, and grinding traces. After masking, the weld bead was clearly isolated as the dominant object, with small gaps closed and background interference significantly reduced. The overlapping bead structure remained intact and visually coherent.
The resulting image presents a clean weld bead with preserved contours and minimal background noise. This output is ready for feature extraction, texture and geometry analysis, weld quality classification, and quantitative evaluation using metrics such as Entropy, SSIM, and GLCM Contrast.

5. Before vs After (Original Grayscale vs Final Masked Result)

Fig. 9. (a) Before original grayscale image, (b) After morphological based processing result

Figure 9 presents a visual summary of the final output produced by the complete morphological-based background suppression pipeline. The comparison between the original grayscale image and the final processed result demonstrates that the weld bead emerges as the dominant structure, with a substantial reduction in background complexity. The sequential application of intensity normalization, adaptive masking, and morphological operations successfully enhances the continuity and visibility of the weld bead while suppressing a large portion of background interference originating from plate textures, oxidation marks, and grinding traces. Nevertheless, residual shadows and fine textural noise remain observable in regions affected by non-uniform illumination and metallic surface reflections. These artifacts indicate that, although the proposed pipeline achieves effective background suppression, complete background removal is not fully attainable using classical morphological processing alone. This visual observation provides an essential qualitative basis for the subsequent quantitative evaluation using entropy, SSIM, and GLCM contrast metrics.

C. *Quantitative evaluation of morphological based background removal*

This study conducted a quantitative evaluation to assess the effectiveness of the proposed morphological-based background suppression stage. The evaluation employed entropy, Structural Similarity Index Measure (SSIM), and Gray Level Co occurrence Matrix (GLCM) contrast to quantify changes in image complexity, structural preservation, and texture separability

TABLE 1. summarizes the quantitative results before and after preprocessing.

Metric	Before Preprocessing	After Preprocessing
Entropy	6.8814	6.5300
SSIM	1.0000	0.7956
GLCM Contrast	58.5352	509.3309

The entropy value decreases from 6.8814 to 6.5300 after preprocessing, indicating a reduction in global image complexity and random background variations. This reduction confirms that the proposed pipeline effectively suppresses background interference rather than merely redistributing pixel intensities. By reducing entropy, the preprocessing stage concentrates visual information on the weld bead region while minimizing irrelevant background elements.

Structural preservation is evaluated using SSIM. The comparison between the original and preprocessed images yields an SSIM value of 0.7956, which indicates a high level of structural similarity. This result demonstrates that the preprocessing pipeline preserves the essential contours and geometric continuity of the weld bead, while introducing controlled structural changes primarily within the background region.

Texture characteristics are analyzed using GLCM contrast. The GLCM contrast value increases significantly from 58.5352 to 509.3309 after preprocessing, indicating enhanced texture separability between the weld bead and the surrounding background. This increase reflects a stronger distinction between object and background textures, which is beneficial for subsequent segmentation and inspection tasks. Overall, the combined reduction in entropy, preservation of SSIM, and increase in GLCM contrast confirm that the proposed morphological-based pipeline achieves effective background suppression while maintaining the structural and textural integrity of the weld bead.

V. Discussion

A. *Effectiveness of the Proposed Preprocessing Pipeline*

The experimental results demonstrate that the proposed preprocessing pipeline is effective in suppressing background interference in weld bead images acquired under complex industrial conditions. The effectiveness of the method is primarily attributed to the synergistic integration of grayscale conversion, intensity normalization, and morphological processing, which together enhance structural discrimination between the weld bead and the surrounding background.

Grayscale conversion plays a fundamental role by eliminating chromatic information and allowing the preprocessing pipeline to focus exclusively on intensity variations that represent spatial structure and object geometry. In weld bead imagery, color information is often inconsistent and does not contribute significantly to shape-based analysis. By operating in the grayscale domain, the proposed method stabilizes the input representation and provides a suitable foundation for subsequent morphological operations, which inherently rely on spatial relationships rather than color cues.

Intensity normalization further enhances the robustness of the pipeline by compensating for non-uniform illumination commonly caused by uneven lighting and metallic surface reflections. Without normalization, regions of the background may exhibit intensity levels similar to those of the weld bead, leading to incomplete suppression or edge distortion during morphological processing. The normalization step reduces global illumination gradients, ensuring that morphological operators act on a more uniform intensity distribution. This

explains the observed reduction in global entropy after preprocessing, as reported in Table 1, indicating decreased background complexity.

Morphological operations, including opening and closing, are then applied to exploit geometric consistency of the weld bead. These operations effectively suppress small-scale background noise and stabilize the continuity of the weld bead structure. The high SSIM value obtained after preprocessing confirms that, despite background suppression, the essential contours and geometric integrity of the weld bead are preserved. At the same time, the significant increase in GLCM contrast demonstrates improved texture separability between the weld bead and the background, making the bead more distinguishable for subsequent inspection tasks.

B. Limitations and Critical Evaluation of Background Suppression

Despite the demonstrated effectiveness of the proposed preprocessing pipeline, the visual comparison between the original and processed weld bead images reveals that background suppression is not fully complete. As shown in the before–after comparison (Figure 9), although the weld bead becomes more prominent after morphological-based processing, strong shadows and residual textural noise on the metallic plate remain visible, particularly in regions adjacent to the weld bead.

The persistence of strong shadows highlights an inherent limitation of morphology based approaches. Morphological operations are designed to operate on local spatial relationships between pixels and do not explicitly model gradual global illumination variations. Consequently, shadowed regions with intensity levels close to those of the weld bead are not reliably distinguished as background and therefore remain partially preserved after preprocessing. This limitation is especially evident in areas affected by non-uniform illumination and specular reflections, where intensity gradients are continuous rather than abrupt.

In addition, high frequency textural noise is still observable in the final output. This indicates that the initial masking and opening–closing operations are not sufficiently selective to fully differentiate between coarse background textures and fine structural details of the weld bead. Importantly, this residual noise should not be interpreted as an implementation error. Instead, it reflects the intrinsic characteristics of weld bead images, which often exhibit complex, non-homogeneous surface textures resulting from grinding marks, material properties, and surface reflections.

From a methodological perspective, these limitations confirm that the proposed approach should be interpreted as a background suppression framework rather than a complete background removal solution. While the pipeline significantly reduces background complexity and enhances weld bead visibility, it does not achieve full object isolation when background textures closely resemble the foreground in both intensity and structure. This critical evaluation aligns with the quantitative findings, where entropy reduction and increased GLCM contrast indicate improved separability, yet SSIM values reveal controlled but non-negligible structural alterations.

VI. Conclusion

The research demonstrates that morphological based background suppression provides a robust and interpretable solution for weld bead imaging under non uniform illumination and metallic reflections, effectively reducing background complexity while preserving the structural and textural integrity of the weld bead. Through the integration of flat field correction, contrast enhancement, adaptive thresholding, morphological opening and closing, and marker controlled, watershed segmentation, the proposed workflow achieved significant entropy reduction, maintained high structural similarity, and enhanced texture separability, confirming its stability and selectivity. Although complete background removal remains challenging when background intensity and texture closely resemble the weld bead, the results validate that this approach offers a reliable foundation for subsequent analytical tasks such as feature extraction and weld quality classification, thereby strengthening the potential of automated inspection systems to deliver consistent and objective weld quality assessment in industrial environments.

VII. Future Work

The remaining shadows, metallic reflections, and background textures observed in the final results indicate limitations of purely morphology-based processing under complex illumination conditions. Future work will integrate illumination-aware modeling, including Retinex based decomposition and flat field correction, to explicitly separate reflectance from illumination and reduce strong shadows. To suppress specular highlights while preserving weld bead boundaries, edge-preserving filtering methods, such as guided filtering and anisotropic diffusion, will be incorporated. Furthermore, to overcome the inability of low-level processing to distinguish weld bead regions from structurally similar backgrounds, a hybrid segmentation framework will be developed, where the current background suppression masks serve as structural priors or weak supervision for semantic segmentation models such as U-Net or attention-based architectures. These extensions aim to achieve more reliable object isolation while retaining the interpretability and stability of the proposed classical pipeline

References

[1] A. Kumar and S. P. Harsha, "A systematic literature review of defect detection in railways using machine vision-based inspection methods," *Int. J. Transp. Sci. Technol.*, vol. 18, no. May 2023, pp. 207–226, 2025, doi: 10.1016/j.ijtst.2024.06.006.

[2] A. A. R. M. A. Ebayyeh and A. Mousavi, "A Review and Analysis of Automatic Optical Inspection and Quality Monitoring Methods in Electronics Industry," *IEEE Access*, vol. 8, pp. 183192–183271, 2020, doi: 10.1109/ACCESS.2020.3029127.

[3] A. Hussain and S. Raza Mehdi, "A Comprehensive Review: 3d Object Detection Based on Visible Light Camera, Infrared Camera, and Lidar in Dark Scene," *Ssrn*, pp. 1–27, 2024, [Online]. Available: https://ssrn.com/abstract=4781073

[4] A. Alhakamy and M. Tuceryan, "Real-time Illumination and Visual Coherence for Photorealistic Augmented/Mixed Reality," *ACM Comput. Surv.*, vol. 53, no. 3, 2021, doi: 10.1145/3386496.

[5] J. Jayanthi and P. U. Maheswari, "Comparative study: enhancing

legibility of ancient Indian script images from diverse stone background structures using 34 different pre-processing methods," *Herit. Sci.*, vol. 12, no. 1, 2024, doi: 10.1186/s40494-024-01169-6.

[6] P. Rodríguez-Gonzálvez and M. Rodríguez-Martín, "Weld Bead Detection Based on 3D Geometric Features and Machine Learning Approaches," *IEEE Access*, vol. 7, pp. 14714–14727, 2019, doi: 10.1109/ACCESS.2019.2891367.

[7] Y. Lin *et al.*, "CLIP is Also an Efficient Segmenter: A Text-Driven Approach for Weakly Supervised Semantic Segmentation," *Proc. IEEE Comput. Soc. Conf. Comput. Vis. Pattern Recognit.*, vol. 2023-June, pp. 15305–15314, 2023, doi: 10.1109/CVPR52729.2023.01469.

[8] H. Rajagopal *et al.*, "Gray level co-occurrence matrix (Glcm) and gabor features based no-reference image quality assessment for wood images," *Proc. Int. Conf. Artif. Life Robot.*, vol. 2021, pp. 736–741, 2021, doi: 10.5954/icarob.2021.os1-1.

[9] M. Al-Khafaji and N. T. A. Ramaha, "Hybrid deep learning architecture for scalable and high-quality image compression," *Sci. Rep.*, vol. 15, no. 1, pp. 1–15, 2025, doi: 10.1038/s41598-025-06481-0.

[10] S. Wang, Z. Li, G. Chen, and Y. Yue, "Weld seam object detection system based on the fusion of 2D images and 3D point clouds using interpretable neural networks," *Sci. Rep.*, vol. 14, no. 1, pp. 1–13, 2024, doi: 10.1038/s41598-024-71989-w.

[11] L. Cai and H. Zhao, "A Multimodal Fusion Method for Weld Seam Extraction Under Arc Light and Fume Interference," *J. Manuf. Mater. Process.*, vol. 9, no. 11, p. 350, 2025, doi: 10.3390/jmmp9110350.

[12] C. Liu, F. Xie, X. Dong, H. Gao, and H. Zhang, "Small Target Detection from Infrared Remote Sensing Images Using Local Adaptive Thresholding," *IEEE J. Sel. Top. Appl. Earth Obs. Remote Sens.*, vol. 15, pp. 1941–1952, 2022, doi: 10.1109/JSTARS.2022.3151928.

[13] M. Mehta and C. Shao, "Federated learning-based semantic segmentation for pixel-wise defect detection in additive manufacturing," *J. Manuf. Syst.*, vol. 64, no. June, pp. 197–210, 2022, doi: 10.1016/j.jmsy.2022.06.010.

[14] J. N. Mlyahilu, J. N. Mlyahilu, J. E. Lee, Y. B. Kim, and J. N. Kim, "Morphological geodesic active contour algorithm for the segmentation of the histogram-equalized welding bead image edges," *IET Image Process.*, vol. 16, no. 10, pp. 2680–2696, 2022, doi: 10.1049/ipr2.12517.

[15] L. Marlinda and M. S. Dewi, "A Morphological Approach for Background Elimination in 2D Images of Buddha Statue Faces," vol. 9, no. 6, pp. 49–55, 2025.

[16] P. Lv, J. Wang, X. Zhang, C. Ji, L. Zhou, and H. Wang, "An improved residual U-Net with morphological-based loss function for automatic liver segmentation in computed tomography," *Math. Biosci. Eng.*, vol. 19, no. 2, pp. 1426–1447, 2022, doi: 10.3934/mbe.2022066.

[17] L. Guo, Y. Yan, J. Cui, and Z. Xu, "Research on Weld Identification and Defect Localization Based on an Improved Watershed Algorithm," *IEEE Access*, vol. 13, no. December 2024, pp. 6869–6877, 2025, doi: 10.1109/ACCESS.2025.3526728.

[18] G. S. Jin, S. J. Oh, Y. S. Lee, and S. C. Shin, "Extracting weld bead shapes from radiographic testing images with u-net," *Appl. Sci.*, vol. 11, no. 24, 2021, doi: 10.3390/app112412051.

[19] D. J. Jobson, Z. U. Rahman, and G. A. Woodell, "A multiscale retinex for bridging the gap between color images and the human observation of scenes," *IEEE Trans. Image Process.*, vol. 6, no. 7, pp. 965–976, 1997, doi: 10.1109/83.597272.

[20] J. B. H. C. Didden, Q. V. Dang, and I. J. B. F. Adan, "Decentralized learning multi-agent system for online machine shop scheduling problem," *J. Manuf. Syst.*, vol. 67, no. February, pp. 338–360, 2023, doi: 10.1016/j.jmsy.2023.02.004.

[21] W. H. Su and S. Y. Chen, "Error-corrected fringe discrimination using nonary-encoded patterns for phase-shifting projected fringe profilometry," *Opt. Lasers Eng.*, vol. 141, no. March 2020, 2021, doi: 10.1016/j.optlaseng.2021.106554.